



Incipient oxidation of Al(111) studied using optical second harmonic generation
by Kejia Wan

A thesis submitted in partial fulfillment of the requirements for the degree of Master of Science in
Physics

Montana State University

© Copyright by Kejia Wan (1989)

Abstract:

Optical second harmonic generation and complementary surface analytical techniques have been used to study the oxidation of the Al(111) surface. Two aspects of the oxidation properties are investigated. The first is the identification of oxide growth phases. When oxygen adsorbs on the Al(111) surface, oxygen bonds initially in two distinct sites such that both a surface phase and a subsurface phase exist on the surface prior to the formation of Al₂O₃. Auger electron spectroscopy, contact potential difference work function measurements and second harmonic generation support this conclusion. Additionally, the second harmonic generation and contact potential difference data indicate that two types of bonds exist between the adsorbed oxygen and the substrate aluminum with increasing exposure. At low oxygen coverage, the bond serves to reduce the density of free electrons of the substrate surface. At higher oxygen exposures, charge transfer occurs from the aluminum to the oxygen atoms. This transfer produces a localized, permanent contribution to the surface dipole moment.

INCIPIENT OXIDATION OF AL(111) STUDIED
USING OPTICAL SECOND HARMONIC GENERATION

by
Kejia Wan

A thesis submitted in partial fulfillment
of the requirements for the degree

of
Master of Science

in
Physics

MONTANA STATE UNIVERSITY
Bozeman, Montana

April, 1989

N378
W1812

APPROVAL

of a thesis submitted by

Kejia Wan

This thesis has been read by each member of the thesis committee and has been found to be satisfactory regarding content, English usage, format, citations, bibliographic style, and consistency, and is ready for submission to the College of Graduate Studies.

22 March 90
Date

Wayne Ford
Chairperson, Graduate Committee

Approved for the Major Department

3/22/90
Date

[Signature]
Head, Physics Department

Approved for the College of Graduate Studies

April 4, 1990
Date

Henry S. Parsons
Graduate Dean

STATEMENT OF PERMISSION TO USE

In presenting this thesis in partial fulfillment of the requirements for a master's degree at Montana State University, I agree that the Library shall make it available to borrowers under rules of the Library. Brief quotations from this thesis are allowable without special permission, provided that accurate acknowledgment of source is made.

Permission for extensive quotation from or reproduction of this thesis may be granted by my major professor, or in his/her absence, by the Dean of Libraries when, in the opinion of either, the proposed use of the material is for scholarly purposes. Any copying or use of the material in this thesis for financial gain shall not be allowed without my written permission.

Signature Kesjia Wan

Date 3/22/90

TABLE OF CONTENTS

	Page
LIST OF FIGURES	v
ABSTRACT	vii
INTRODUCTION	1
DESCRIPTION OF EXPERIMENTAL TECHNIQUES.....	3
Apparatus	3
Sample Preparation	12
Auger Electron Spectroscopy.....	15
Contact Potential Difference Measurement	22
Surface Second Harmonic Generation	31
EXPERIMENTAL RESULTS	38
Auger Electron Spectroscopy.....	38
Contact Potential Difference Measurements	41
Surface Second Harmonic Generation Measurements.....	45
DISCUSSION	49
Oxidation of Al (111).....	49
Incipient Oxidation Process.....	56
Summary and Final Considerations	63
REFERENCES CITED	65
APPENDIX	70
Computer Interface	71

LIST OF FIGURES

Figure	Page
1. Schematic description of the ultra high vacuum experimental chamber.....	4
2. Experimental view of the sample holder.....	5
3. Second harmonic generation experimental configuration.....	8
4. Schematic description of beamsizer reducer.....	9
5. Boxcar electronic setup.....	9
6. Auger spectrum of sample before (a) and after (b) cleaning.....	14
7. Schematic of Auger process.....	16
8. Auger cross section as a function of primary beam energy.....	21
9. Effect of the surface on the binding energy of an electron.....	24
10. Schematic of contact potential difference method.....	26
11. Schematic of two capacitor model for CPD measurements.....	28
12. Two capacitor model results for CPD measurements.....	29
13. Measured dependence of CPD with sample-probe distance.....	30
14. Schematic of SHG measurements.....	32
15. O ₂ /Al(111) Auger uptake.....	39
16. Auger oxygen uptake.....	40
17. Kelvin probe result.....	42

LIST OF FIGURES (Continued)

18. Stop oxygen exposure the work function response.	44
19. SHG results p-polarized incident.	46
20. SHG results s-polarized incident.	47
21. SHG results for sputtering surface.	48
22. Finite well model for the surface electrons, work function (a) Φ_I and (b) Φ_{II}	62
23. Diagram of computer programs.	73
24. Software listing.	74

ABSTRACT

Optical second harmonic generation and complementary surface analytical techniques have been used to study the oxidation of the Al(111) surface. Two aspects of the oxidation properties are investigated. The first is the identification of oxide growth phases. When oxygen adsorbs on the Al(111) surface, oxygen bonds initially in two distinct sites such that both a surface phase and a subsurface phase exist on the surface prior to the formation of Al_2O_3 . Auger electron spectroscopy, contact potential difference work function measurements and second harmonic generation support this conclusion. Additionally, the second harmonic generation and contact potential difference data indicate that two types of bonds exist between the adsorbed oxygen and the substrate aluminum with increasing exposure. At low oxygen coverage, the bond serves to reduce the density of free electrons of the substrate surface. At higher oxygen exposures, charge transfer occurs from the aluminum to the oxygen atoms. This transfer produces a localized, permanent contribution to the surface dipole moment.

INTRODUCTION

The oxidation of aluminum is of fundamental importance to both basic scientific research and industrial applications. Alumina is the fully oxidized form of aluminum and is widely used as support material in industrially invaluable bimetallic catalysts. Hence, the commercial importance of alumina provides a practical stimulation for basic studies of aluminum oxidation. One goal of basic research in this area is the microscopic description of the formation and chemical activity of the oxidized surface. In this manner, properties of the surface such as structure and composition might be related to specific catalytic properties.¹ Ultimately, it is envisioned that catalysts with desired activities and specificities can be designed and manufactured.

Microscopic studies of the oxidation process have utilized a wide variety of surface sensitive techniques. These include: low energy electron diffraction (LEED), photoemission experiments, contact potential difference work function measurements (CPD), Auger electron spectroscopy (AES) and electron energy loss spectroscopy. Batra and Kleinman have published a comprehensive review of this literature.² Nevertheless, the oxidation of aluminum still presents many controversial issues. The most studied surface is Al(111). Different authors have drawn different conclusions regarding the oxidation mechanism for the (111) surface. Some claim that surface and subsurface phases occur in a distinct sequence, while others have concluded that the two phases always coexist.²

This thesis proposes a new description of the incipient oxidation of Al(111) using the experimental techniques of AES, CPD, and a recently developed technique called surface enhanced second harmonic generation (SHG).³ The SHG technique specifically emphasizes the changes in electronic structure and the concomitant changes of the surface bonding that occur during the oxygen exposure. At very low exposures molecular oxygen dissociates at the clean surface. The oxygen adatoms provide a decrease in the density of states of the electrons at the surface for

energies near the Fermi level but no significant charge transfer occurs. Thus, for coverages up to 0.1 monolayer (ML) the oxygen adatom is in a "metallic" chemisorption bond. At higher coverages charge is localized in the Al-O bonds and charge transfer of electrons into the electronegative oxygen occurs. Ionic bonding begins at 0.1 ML and dominates with increasing coverage. Thus, with increasing oxygen coverage the chemisorption bond converts from metallic to ionic in character.

DESCRIPTION OF EXPERIMENTAL TECHNIQUES

Apparatus

The experimental apparatus used in our experiments is part of the surface science laboratories at the Physics Department of Montana State University. It consisted of two parts: an ultra high vacuum (UHV) surface science chamber and a pulsed nanosecond laser source and optical system.

The stainless-steel UHV chamber was once part of a Physical Electronics PHI-545 Scanning Auger Microprobe. The chamber was pumped by a 220 L/sec ion pump, a Leybold-Heraeus 150 L/sec turbomolecular pump, and a titanium sublimation pump. After a 24-hour, 140 C bake-out the base pressure of the system was routinely 1.5×10^{-10} torr. A schematic diagram of this apparatus is presented in Figure 1.

Argon and oxygen, purchased from Matheson Gas Products Inc. with purity of 99.9995% for argon and 99.99% for oxygen, were leaked into the chamber during the experiments, using separate Varian model 951-5106 leak valves. The gas manifold system, displayed in Figure 1, is designed to store the gases separately and can be pumped out using the turbomolecular pump after first closing the UHV gate valve to the main chamber. The argon gas reservoir was trapped with liquid nitrogen to reduce the water impurity level of the gas. Argon was used to clean the sample by ion bombardment. The sample was exposed to oxygen by backfilling the chamber with flowing oxygen to the desired pressure. Before introducing the gases into the chamber, the ion pump was valved closed for protection from back-contamination from the pump and the chamber pumped using only the turbomolecular pump. During experiments, the pressure was recorded by a bare ion gauge. This gauge was not in proximity nor in line of sight to the sample so as to prevent excited oxygen from hitting the sample. A voltage meter was used to extend the precision of the pressure reading so as to more precisely control the exposure rate.

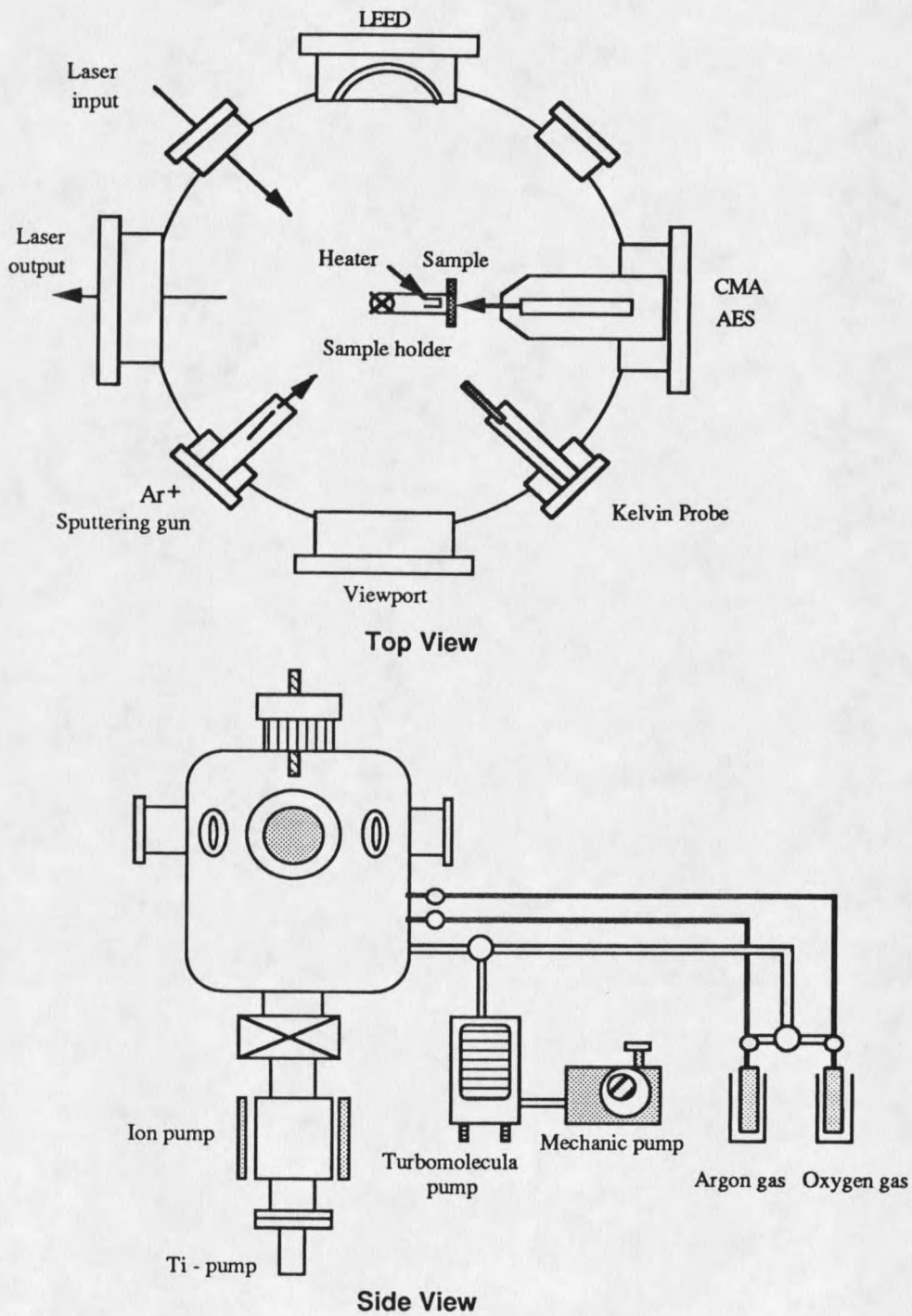


Figure 1. Schematic description of the ultra high vacuum experimental chamber; used in the experimental measure.

The sample was heated during the surface cleaning process using an electron beam heater. This heating scheme is shown in Figure 2. The sample was mounted above a hollow cylinder 1/2 inch in diameter. Inside this cavity a 0.05 inch tantalum filament was resistively heated to provide an electron source. A tantalum foil cylinder encircled and was connected electrically with the filament. The sample was held at ground potential and the filament floated at a high negative potential. The typical operating voltage on the filament was negative 1000 V, which produced a 4-mA emission current. This heating arrangement gave good temperature control and allowed heating from room temperature to 430 C in less than 5 minutes. Between heating cycles the rigidity of this sample holder kept the sample in a stable position, an essential requirement to retain a reproducible optical alignment for the second harmonic generation experiments.

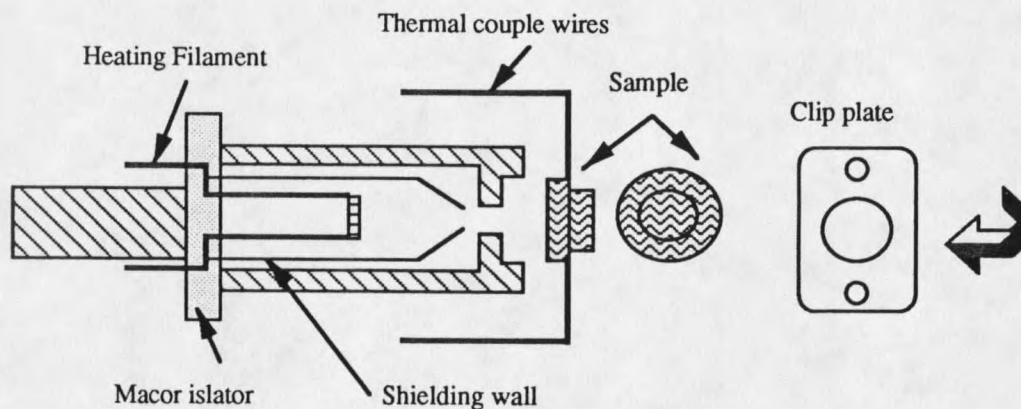


Figure 2. Experimental view of the sample holder.

Auger electron spectroscopy (AES) was used to monitor the sample surface contamination prior to making each oxygen exposure. We used a single pass cylindrical mirror analyzer (CMA) with an integral gun, operated in the low resolution modulated pass energy mode. In this mode, a computer utilized the digital to analog converter in the Stanford Research System Model SR510

lock-in to generate a ramp voltage V_S with a prescribed lower limit, upper limit, and sweep rate. The ramp voltage was modulated by a sinusoidal wave generated by the reference signal output of the SR510 lock-in, typically of 1.6 V peak to peak at a frequency of 4.07 KHz. The voltage V_S was connected to the V_m input of the CMA which is connected internally to the outer cylinder. The inner cylinder was grounded. The pass energy of the analyzer E is proportional to V_m . This relationship was taken to be that given by the operation manual,⁴ $E = 1.76 V_m$, where E is in electron volts and V_m is in volts. The exact value of the analyzer constant (1.76) depends on the structural geometry of the CMA and the work function variation in the system. Subsequent measurements of this system suggest that the proportionality value should be 1.72. However, this error leads only to a small and unimportant general shift of the peak energies. The CMA and associated control electronics derived from the original PHI 545 scanning Auger microprobe.

A Varian LEED unit was also available on the chamber. It consisted of the Varian LEED optics, a coaxial electron gun, model number 981-2145, and LEED control unit, model number 981-2148. LEED was routinely used to monitor the cleaning and annealing of the sample by checking surface orientation. It is also capable of performing AES.

A Delta-Phi Electronic Model 05 Kelvin probe was used to measure the change in work function of the sample during oxygen exposure. The probe used for the measurements was a molybdenum paddle mounted on a piezoelectric crystal. The assembly was driven to oscillate at its resonant frequency near 170 Hz by the Kelvin Control Unit. The change of work function was measured in two ways. As purchased, the Kelvin probe control unit contained a lock-in amplifier and oscillation feedback circuit. The work function difference between sample and paddle, or CPD, is available as a separate output of the control unit. This CPD reading was digitized and stored in a microcomputer as a function of exposure time. In second method, an alternative instrumentation setup was used to eliminate a voltage drift associated with Kelvin control unit and to improve the signal-to-noise. In this case the lock-in amplifier of the Kelvin probe control unit

was replaced by the SR510. However, no significant differences in the CPD measurements were found using the two methods.

Measurement of the SHG signal was performed using the experimental arrangement shown in Figure 3. The laser was a pulsed Q-switched mode-locked neodymium-doped yttrium aluminum garnet (Nd:YAG) laser, a Spectra-Physics Quanta-Ray[®] DCR-3. It provided light pulses at a wavelength of 1.06 μ . Although the pulse full width at half maximum was rated at between 7 and 9 ns by the manufacturer, we operated in a low power mode that provided pulses of about 15 ns at 1.06 μ with a repetition rate of 10 hz. A second harmonic component was uncontrollably generated within the laser cavity and had to be blocked by a dielectric mirror chosen to allow transmission only of the main 1.06 μ component.

Variation of the laser intensity was monitored using a reference signal, channel B in Figure 3. This reference signal was generated by reflecting twenty percent of the incident beam through a quartz quarter wave plate as indicated in Figure 3. The reference signal was detected using a photomultiplier tube (PMT), after passing through a BG-18 filter to the block 1.06 μ beam. Some plastic neutral density filters were used to further reduce the signal intensity.

The remaining eighty percent of original 1.06 μ beam was directed into the experimental chamber. The SH signal produced in this beam was directed to channel A in the electronics. Dielectric mirrors optimized for reflecting 1.06 μ light were utilized to direct the beam onto the sample. Before the beam was incident into the chamber, a Fresnel rhomb polarizer was used to select the desired polarization with respect to the incident plane of the sample.

The laser produced a diffraction-limited spot size of about 9 mm diameter. In order to have a smaller, nondivergent beam at the sample, a beam size reducer was built using two thin lenses, a converging and a diverging as illustrated in Figure 4. The ratio of the input and output beam diameters w_1 and w_2 can be determined by simple plane geometry resulting in the relation:

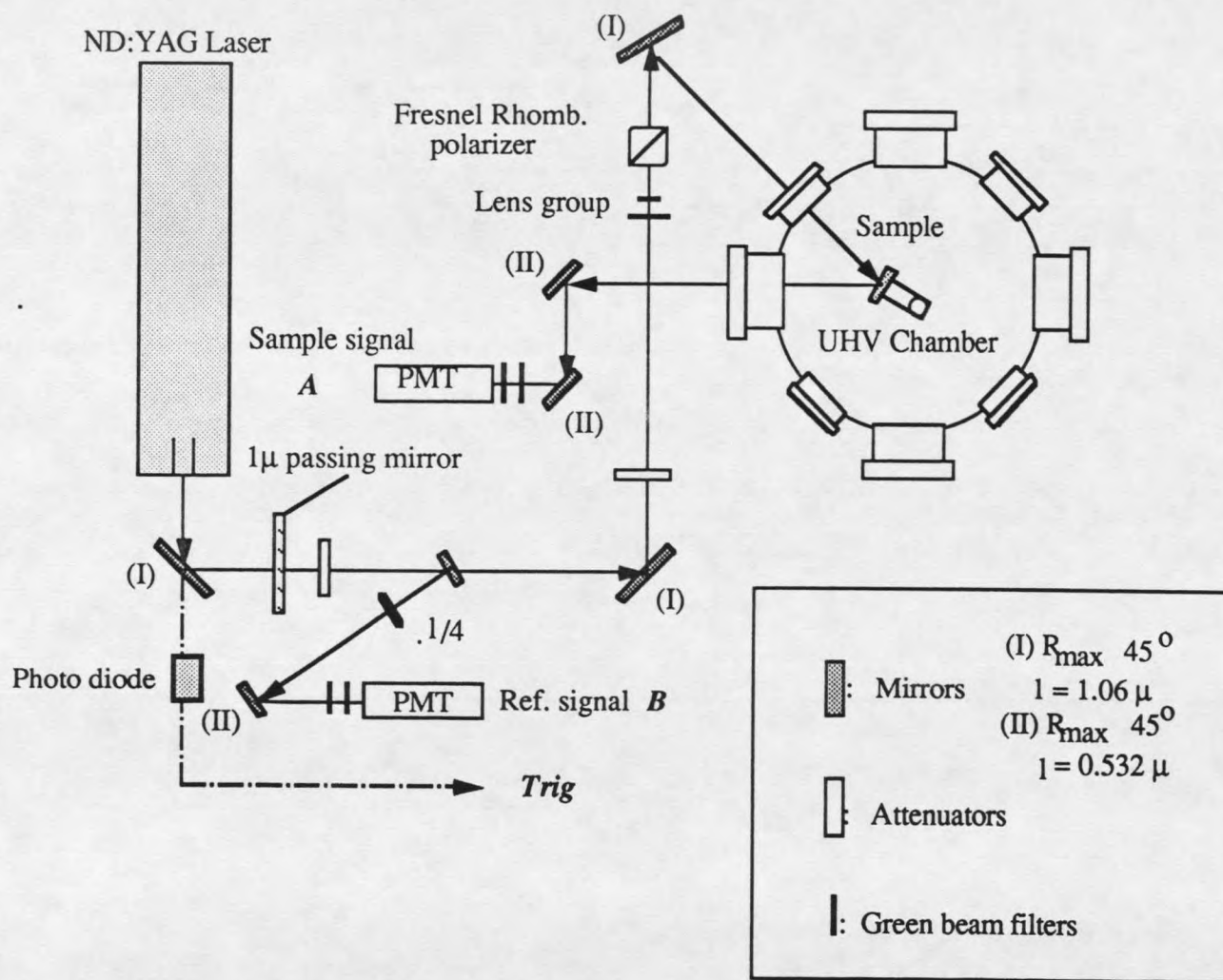


Figure 3: Second harmonic generation experimental configuration

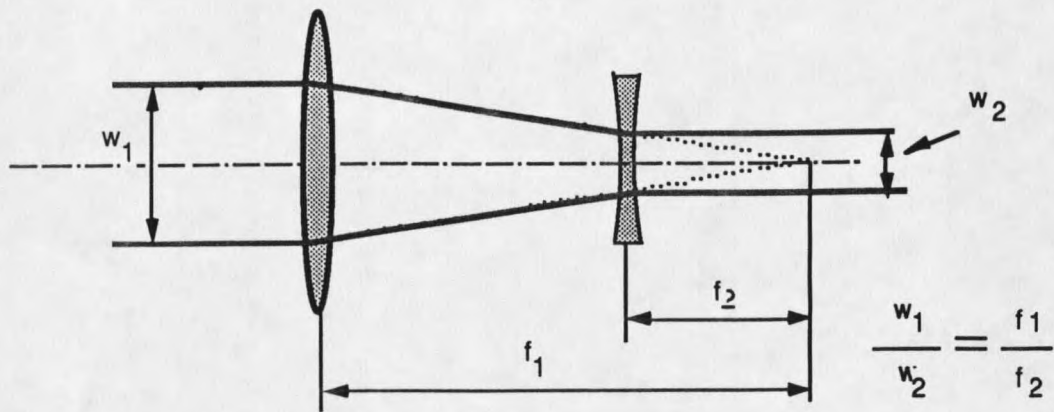


Figure 4. Schematic description of beamsize reducer.

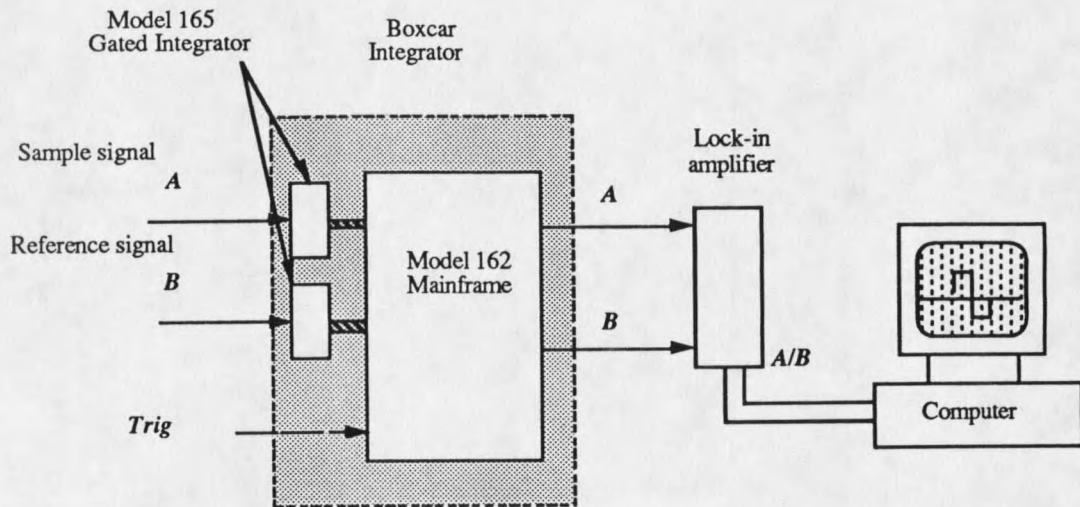


Figure 5. Boxcar electronic setup.

$$\frac{w_1}{w_2} = \frac{f_1}{f_2}. \quad (1)$$

The choice of the beam size was accomplished by appropriate selection of focal lengths. In our experiment, we needed the beam size of about 2.5 mm diameter. Thus, we chose $f_1 = 200$ cm and $f_2 = 50$ cm.

The beam was then directed into the experimental chamber through a zero-length 7056 glass/Kovar viewing window attached to a 2.75" Conflat[®] flange. The light was incident on the sample at an angle of 30°. The reflected 1.06 μ and the surface generated 0.532 μ second harmonic light were collinear from the sample, although some unwanted diffuse scattering occurred, indicating that the sample was not polished optically flat or smooth. The reflected beam exited the chamber through a similar glass window. The 1.06 μ beam was filtered from the signal optical path using two dielectric mirrors which reflected only the 0.536 μ light. Further spectral filtering of this light was performed with a KG-3 filter before it entered the second PMT.

The electronic instrumentation consisted of a pair of photomultiplier tubes (model RFI/S MK 11) from Thorn EMI Gencom Inc., a pair of Model 165 gated integrators and a Model 162 boxcar from EG&G Princeton Applied Research.⁵ The boxcar signal-averaging technique is standardly used when making measurements of a pulsed nature to increase the signal to noise ratio. The electronics of this measurement are outlined in Figure 5. The sample signal was weaker than the reference signal and needed to be amplified by a factor of 10 prior to signal processing. In order to accommodate the time delay internal to the boxcar, both sample and reference signals were delayed by 75 ns before entering the boxcar. The boxcar samples the input signals with a time width aperture that can be fixed independently at any point on each of the input signal waveforms. The boxcar integrates each signal within its time aperture using a preselected, variable time constant. The output of integrator is the average of large number of repetitions of the input signal

over the aperture duration. In our experiment we used an integrating time constant of 100 μ s and an aperture duration of 50 ns, yielding analog signal averaged over about 130 pulses.

The Model 165 Gated Integrator module is a plug-in module for the Model 162 boxcar. Its full-scale signal-sensitivity is adjustable in seven steps, from ± 50 mV to ± 5 V, to accommodate a wide range of input-signal and noise levels. In our experiments, the sensitivity setting was chosen from 100 mV to 250 mV according to the signal magnitude.

The Model 162 mainframe contains the primary timing and control functions, as well as the output signal-processing circuitry. There is provision for supplying the gated-and-averaged signal from either channel to the mainframe output. Alternatively, one can select the difference between the two signals at the mainframe output. We used both channels connected with the model 165 gated integrator. With the addition of optional signal-processing circuit cards, the model 162 can provide an output consisting of the product, ratio, or log of the ratio of the two independent output channels. The mainframe output signal can be smoothed by a low-pass filter. In our experiment, two outputs of the integrators were directly connected to the ancillary analog-to-digital converters of the SR510 Lock-in so that we could digitize each channel in real time. Front-panel delay controls are provided on the boxcar that permit the aperture in each channel to be delayed independently from about 5% to 100% of the delay range, selectable in 1-2-5 sequence from 0.1 μ s to 50 ms. The boxcar output of each channel was normally optimized by adjusting the delay so as to best position the integrating window over the signal pulse. This value was typically 200 ns for our experimental configuration.

The output sample and reference signals channels A and B were digitized using two A/D converters contained in SR510 lock-in amplifier. The digitized signals were read by computer which also plotted the ratio of the sample signal to the reference signal. Performing this division was necessary to eliminate the effect of laser fluctuations. The computer was instructed to accumulate two or three points within the time constant of the boxcar electronics.

All the above measurements were controlled by an ATT 6300+ computer. A Stanford Research System Model SR510 lock-in amplifier, which provides a lock-in amplifier and D/A and A/D functions, was used as an interface between the computer and experimental hardware. The software control system was developed by adapting a general purpose experimental control program written by William Hough, an MSU undergraduate research assistant. When performing AES measurements, the lock-in output was recorded as a function of the electron kinetic energy. This output is proportional to the derivative of the Auger intensity with the CMA operating in the modulated pass energy mode. When performing Kelvin probe work function measurements using the standard configuration, the nulling voltage equal to the negative of the CPD, as described below, was measured as a function of time. In the second method of CPD measurements in which the SR510 is used, the lockin output was first calibrated to a known externally applied nulling voltage and this calibration used to translate the changes in lockin output with required nulling voltage during the measurements. That is, no nulling voltage is applied to the Kelvin probe in this approach. When performing second harmonic generation measurements, the SHG intensity was divided by the reference signal and then was plotted vs oxygen exposure as for the Kelvin probe measurements. The computer program is described in the appendix.

Sample Preparation

In general, the initial oxidation of the Al(111) surface has been shown to be strongly dependent upon surface geometry and surface condition,² the preparation of the sample being an important process. Several factors that might influence the surface preparation are the sample polish, the chemical etching process, the energy of argon ions for bombardment, and the annealing procedure.

The Al(111) single crystal sample with a purity greater than 99.999% was purchased from the Monocrystal Corporation of Cleveland, Ohio. The surface normal was determined to be within

